JOURNAL OF OPTOELECTRONICS AND ADVANCED MATERIALS Vol. 16, No. 3-4, March - April 2014, p. 333 -339

Study towards high efficiency CdS/CdTe solar cells

H. A. MOHAMED[a,b]
[a]*Physics department, Faculty of Science, Sohag University, 82524 Sohag, Egypt.*
[b]*Physics department, Teachers College, King Saud University, 11148 Riyadh, KSA.*

The effect of CdS thickness and CdTe resistivity on short-circuit current, open-circuit voltage, fill factor and cell efficiency is studied in this work. The results have been carried out based on the optical losses (reflection and absorption) and recombination losses (front and back) under certain parameters of the absorber layer. It has been found that the optical losses decrease with reducing the thickness of CdS layer. At CdS thickness of 100 nm, the contribution of optical and recombination losses is about 35% where the recorded current density is 20.1 mA/cm^{-2}. With further decrease in CdS thickness up to 70 nm, the short-circuit current density increases up to 21.1 mA/cm^{-2} where the contribution of these losses is about 32%. The output power, open-circuit voltage and fill factor of CdS/CdTe solar cell are determined from the *J-V* characteristic. It has been found that these parameters increase with decreasing the resistivity of CdTe absorber layer and thinning the CdS window layer. The maximum cell efficiency of 16.5 % is obtained at CdTe resistivity=0.1 Ω cm and CdS thickness=70 nm.

(Received September 7, 2013; accepted March 13, 2014)

Keywords: Optical and recombination losses, CdTe resistivity, CdS thickness, CdS/CdTe solar cells efficiency.

1. Introduction

Thin film photovoltaic solar cells, in particular CdS/CdTe, are extremely prospective for the large-scale production of solar modules for space and terrestrial applications. For the past two decades, intensive research aimed toward increasing the efficiency of CdS/CdTe devices have been carried out by scientists and engineers worldwide. These efforts are aimed toward improving the quality of the CdTe and CdS layers [1-4], reducing the optical losses [5], perfecting the rear contact [6, 7], variation of the doping concentration in the materials [8, 9], and many other problems.

Today the challenge facing the researchers and technologists is how to increase the efficiency of CdS/CdTe cells from the current efficiency of 16–17% [10, 11] and to decrease the gap between actual efficiency and the theoretical limit of 28–30% [12, 13]. It is known that the efficiency of CdS/CdTe solar cells depends on short-circuit current (J_{SC}), open-circuit voltage (V_O), and fill factor (FF). After considering the recombination losses (front and pack) and optical losses in the CdTe cell (reflection of the interfaces air-glass, glass-ITO, ITO-CdS and CdS-CdTe and absorption in CdS and CdTe layers.), all components of J_{SC} appear to be accounted for, and this quantity is close to its practical limit [5, 14-16]. To increase the efficiency of thin film CdS/CdTe solar cells both the fill factor (FF) and open-circuit voltage (V_O) must be improved.

This work studies the effect of CdS thickness and CdTe resistivity on short-circuit current, open-circuit voltage, fill factor and cell efficiency of CdS/CdTe solar cells. The results have been carried out based on the optical losses (reflection and absorption) and recombination losses (front and back) under certain parameters such as: CdS thickness; electron and hole lifetime; recombination velocity; concentration of uncompensated acceptors and diffusion coefficient.

2. Transmission spectrum

Before reaching the photoelectrically active CdTe absorber layer, solar radiation penetrates the glass plate, a layer of transparent conducting oxide (TCO) and CdS window layer. Obviously, this is accompanied by optical losses upon reflection from the following interfaces: air–glass, glass–TCO, TCO–CdS, and CdS–CdTe, and absorption in TCO and CdS. Therefore, the transmission coefficient $T(\lambda)$ due to optical losses is given by [17].

$$T(\lambda)=(1-R_{12})(1-R_{23})(1-R_{34})(1-R_{45})(e^{-\alpha_1 d_1})(e^{-\alpha_2 d_2}) \quad (1)$$

where R_{12}, R_{23}, R_{34}, R_{45} is the reflectivity of the interfaces air-glass, glass-ITO, ITO-CdS and CdS-CdTe, respectively. α_1, α_2, d_1, d_2 is the absorption coefficient and thickness of ITO and CdS layers, respectively. The effect of multiple reflections and related interference are not taken into calculations owing to a minor error contributions in the calculation of short-circuit current [5, 16].

Fig.1 shows the calculated transmission of glass/ITO/CdS at various values of CdS thickness (70, 80, 90 and 100 nm). These results are carried out at 100 nm thickness of ITO layer. It is known, however, that it is difficult to obtain uniform and pin-hole free CdS layers thinner than 50 nm [5], therefore the CdS thickness is assumed in the range 70-100 nm. Besides, Korevaar et al[18] reported that CdS with a thickness of 80 nm is considered a better choice to increase the CdS/CdTe efficiency up to 16% due to increasing the open-circuit voltage and fill factor.

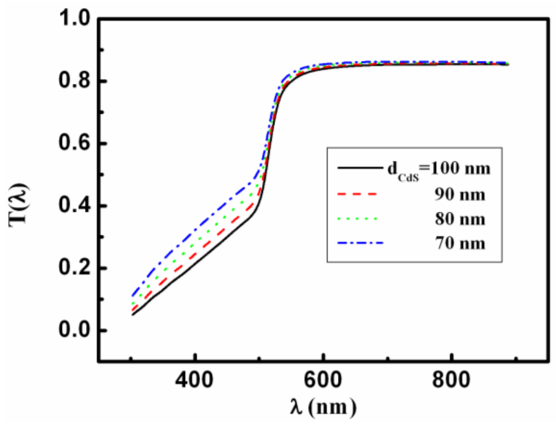

Fig.1. Calculated transmission (T) as a function of wavelength (λ) due to reflection and absorption losses at different values of CdS thickness.

The calculation of reflection and absorption coefficient was studied in details in refs. [15, 16]. As can be seen from this figure the transmission increases with decreasing the thickness of CdS. The optical losses are about 14 % in the wavelength range 550-850 nm. Much more losses are observed in the wavelength region < 500 nm which mainly caused by absorption losses in ITO and CdS layers [15]. By thinning the CdS layer from 100 to 70 nm, it is possible to reduce the optical losses by 5% in the wavelength range 500-600 nm.

3. Short-circuit current

One of the essential factors which is used in calculating the current density is the quantum efficiency η_{int}. It is reported [13, 16] that the quantum efficiency is consisted of two components, the first is called drift photoelectric quantum yield (η_{drift}) and the second one is called diffusion (η_{dif}). Those two components are given by [19]:

$$\eta_{drift} = \frac{1 + \frac{S}{D_P}\left(\alpha + \frac{2}{W}\frac{\varphi_0 - qv}{kT}\right)^{-1}}{1 + \frac{S}{D_P}\left(\frac{2}{W}\frac{\varphi_0 - qv}{kT}\right)^{-1}} - \exp(-\alpha W) \quad (2)$$

$$\eta_{dif} = \frac{\alpha L_n}{\alpha^2 L_n^2 - 1}\exp(-\alpha W) \times$$
$$\left\{ \alpha L_n - \frac{\frac{S_b L_n}{D_n}\left[\cos\left(\frac{d-W}{L_n}\right) - \exp(-\alpha(d-W))\right] + \sinh\left(\frac{d-W}{L_n}\right) + \alpha L_n \exp(-\alpha(d-W))}{\frac{S_b L_n}{D_n}\sinh\left(\frac{d-W}{L_n}\right) + \cosh\left(\frac{d-W}{Ln}\right)} \right\} \quad (3)$$

where S is the velocity of recombination at the front surface, S_b is the recombination velocity at the back surface of CdTe layer, D_p is the diffusion coefficient of holes, W is the width of the space-charge region in the CdS/CdTe, α is the absorption coefficient of CdTe at a given wavelength, φ_0 is the barrier height at the semiconductor side, v is the applied voltage, q is the electron charge, k is the Boltzmann constant, d is the thickness of CdTe, $L_n=(\tau_n D_n)^{1/2}$ is the electron diffusion length, τ_n and D_n are the electron lifetime and diffusion coefficient, respectively.

Equation (2) takes into account the surface recombination at the CdS-CdTe interface (front recombination), while equation (3) takes into account the recombination at the back surface of the CdTe layer (back recombination).

The width W of space-charge region (depletion layer) which is mainly depending on the concentration of uncompensated acceptors (N_a - N_d) (the total concentration of acceptors minus the total concentration of donors) is given by [19]:

$$W = \sqrt{\frac{2\varepsilon\varepsilon_0(\varphi_0 - qv)}{q^2(N_a - N_d)}} \quad (4)$$

where ε is the relative permittivity of the semiconductor, ε_0 is the permittivity of free space and (N_a-N_d) is the concentration of uncompensated acceptors in the CdTe layer.

In the present calculations, N_a-N_d= 10^{16} cm^{-3}, ε=10.6, S=10^7 cm/s, τ_n=10^{-9} s, D_n=25 cm^2/s, D_p=2 cm^2/s, and d=5 μm.

Fig.2 represents the quantum efficiency spectra calculated using equations (2), (3) and (4) at different values of applied voltage. It is clear that the drift component of quantum efficiency decreases with increasing the applied voltage and an opposite manner can be observed in the cause of diffusion component.

The obtained expressions for quantum efficiency spectra can be used to calculate the short-circuit current density J_{SC} using the following equation. The calculations will be done for AM1.5 solar radiation using Tables ISO 9845-1:1992 (Standard ISO, 1992) [20].

$$J_{SC} = q\sum_i T(\lambda)\frac{\phi_i(\lambda_i)}{h\nu_i}\eta(\lambda_i)\Delta\lambda_i \quad (5)$$

where $T(\lambda)$ is the optical transmission, Φ_i is the spectral power density ($mWcm^{-2}\mu m^{-1}$), $\Delta\lambda_i$ is the interval between the two neighboring values λ_i, and η ($\eta = \eta_{drift} + \eta_{dif}$) is the total quantum yield of photoelectronic conversion in the CdTe absorber. Let us first consider the drift component of the short-circuit current density (J_{drift}) which is calculated by Eqs. (2) and (5). Fig. (3-a) shows the calculation results for J_{drift} depending on the applied voltage. This figure represents that the drift component of short-circuit current gradually decreases with increasing V and approaches a minimum value of J_{drift}= 12 mA/cm^2 at V=0.9 volt. Besides, using Eqs. (3) and (5), the diffusion component of the short-circuit current density (J_{dif}) is estimated and its values are plotted in figure (3-a) as a function of applied voltage. It is obvious that J_{dif} increases with V and approaches a maximum value of 7.9 mA/cm^2 at V=0.9 volt. Decreasing the drift component of the short-circuit current density with increasing the applied voltage can be attributed to the decreasing of drift component of spectral quantum efficiency with applied voltage as shown in Fig. (2-a). This behavior indicates that the surface recombination increases with increasing the applied voltage and this maybe due to a significant portion of radiation is absorbed outside the space charge region. While the increasing of the diffusion component of the short-circuit current density with increasing the applied voltage is due to increasing the diffusion component of spectral quantum efficiency as shown in Fig. (2-b) and hence decreasing the back recombination effect.

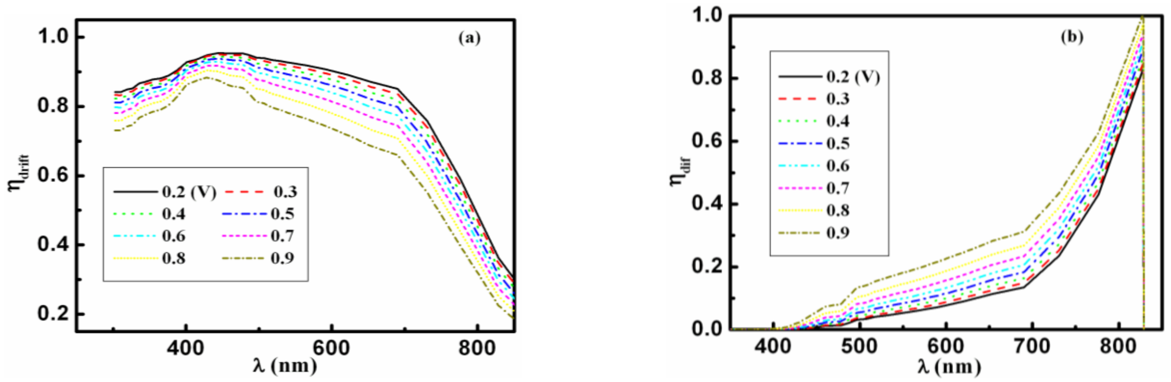

Fig. 2. Drift η_{drift} (a) and diffusion η_{dif} (b) photoelectric quantum yield spectra at different values of applied voltage.

Fig. (3-b) shows the total calculated short-circuit current J_{sc} (the sum of the drift and diffusion components) as a function of space-charge width (W) at different thicknesses of CdS layer. One can see that when the CdS thickness decreases from 100 nm to 70 nm, the short-circuit current density increases from 19.93 to 20.1 at W=0.2 μm and slight increase in the current density can be observed with further increase in W. On the other hand, this figure indicated that the optical (reflection and absorption) and recombination (front and back) losses are about 35 % at d_{CdS}= 100 nm. Where, the maximum value of current density (J^0_{SC} = 31.12 mA/cm^2) decreases to 20.1 mA/cm^2 and these losses become 32 % at d_{CdS}= 70 nm.

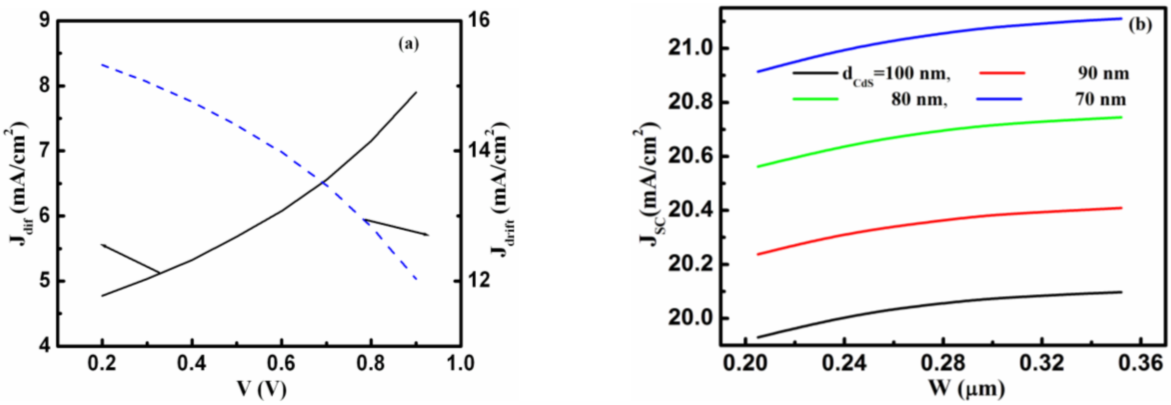

Fig. 3. Drift (J_{drift}) and diffusion (J_{dif}) components of the short-circuit current density as a function of applied voltage (V) (a) and the total short-circuit current density (J_{SC}) as a function of space charge width (W) at different values of CdS thickness (b).

4. J-V characteristic

In this section, the dependences of the open-circuit voltage(V_o), fill factor(FF), output power (P) and efficiency (η %) of a CdS/CdTe solar cell on the resistivity of the CdTe absorber layer and CdS thickness will be investigated with the aim to optimize these parameters and hence to improve the solar cell efficiency. The above parameters can be determined from the J-V characteristic under illumination which can be presented as:

$$J(V) = J_d - J_{ph} \tag{6}$$

where $J_d(V)$ is the dark current density and J_{ph} is the photocurrent density. In most papers, the analytical description of J–V characteristics have been done using a semi-empirical formula for the dark current density in the so-called “ideal” solar cell which is described by the Shockley equation:

$$J_d(V) = J_S \left[\exp\left(\frac{qV}{kT}\right) - 1\right] \tag{7}$$

where J_s is the saturation current density equals the reverse current independent on the voltage V as qV is higher than a few kT. In this work, the measured J–V characteristics of CdS/CdTe heterostructure are governed by the generation-recombination Sah–Noyce–Shockley theory [21-23]. The Sah-Noyce-Shockley theory supposes that the generation-recombination rate in the section x of the space-charge region is determined by expression [21]:

$$U(x,V) = \frac{n(x,V)P(x,V) - n_i^2}{\tau_{Po}[n(x,V) + n_1] + \tau_{no}[P(x,V) + P_1]} \tag{8}$$

where τ_{no} and τ_{po} is the effective lifetime of electrons and holes in the depletion region, respectively, n_i is the intrinsic carrier concentration and the values n_1 and P_1 are determined by the energy spacing between the top of the valence band and the generation-recombination level E_t, i.e.

$$P_1 = N_V \exp(-(E_t/kT)) \tag{9}$$

$$n_1 = N_C \exp(-(E_g - E_t)/kT) \tag{10}$$

where N_c and N_v is the effective state densities in the conduction and valence bands, respectively and given by:

$$N_C = 2\left(\frac{m_n KT}{h^2}\right)^{3/2}, \quad N_V = 2\left(\frac{m_p KT}{h^2}\right)^{3/2} \tag{11}$$

In this equation, m_n and m_p are the effective masses of electrons and holes.

The values $n(x, V)$ and $P(x, V)$ in Eq. (8) are the carrier concentration in the conduction and valence bands and given by [22].

$$P(x,V) = N_C \exp\left[-\frac{\Delta\mu + \varphi(x,V)}{kT}\right] \tag{12}$$

$$n(x,V) = N_v \exp\left[-\frac{E_g - \Delta\mu - \varphi(x,V) - qV}{kT}\right] \tag{13}$$

where $\Delta\mu$ is the energy spacing between the Fermi level and the top of the valence band of CdTe and $\varphi(x, V)$ is the electron energy in the space charge region is given by:

$$\varphi(x,V) = (\varphi_0 - qV)\left(1 - \frac{x}{W}\right) \tag{14}$$

According to the Eqs.(8-14), the recombination-generation current are found by integration of $U(x, V)$ throughout the entire depletion layer [13]:

$$J_{gr} = q\int_0^W U(x,V)\,dx \tag{15}$$

On the other hand, since in CdS/CdTe junction the barrier for holes is higher than that for electrons, the electron component dominates the over-barrier current. Obviously, the electron flow current in analogous to that occurring in the p-n junction and one can write for the over-barrier current density [12]:

$$J_n = = q\frac{n_p L_n}{\tau_n}\left[\exp\left(\frac{qV}{kT}\right) - 1\right] \tag{16}$$

where n_p is the concentration of electrons in the bulk part of the p-CdTe layer, given by:

$$n_P = N_C \exp\left(-\frac{E_g - \Delta\mu}{kT}\right) \tag{17}$$

Thus, according to the above-presented, the dark current density in CdS/CdTe heterostructure $J_d(V)$ is the sum of the generation-recombination and over-barrier components:

$$J_d(V) = J_{gr}(V) + J_n(V) \tag{18}$$

The relation between $\Delta\mu$ and the resistivity of CdTe (ρ) can be written in the form [24]:

$$\Delta\mu = kT \ln\left(\frac{1 - \sqrt{1 - 4q^2\mu_n\mu_p n_i^2\rho^2}}{\frac{2q\mu_n n_i^2\rho}{N_V}}\right) \quad 19)$$

where μ_n=1000 cm^2/V.s, μ_p=80 cm^2/V.s is the electron and hole mobility in CdTe layer, respectively.

In Fig. 4 the calculated J-V characteristics of the CdS/CdTe heterojunction are shown. The curves have been calculated by Eq. (6) using Eqs. (7)-(19), for various resistivities of the p-CdTe layer at d_{CdS}= 100 and 70 nm. In these calculations, the short-circuit current density was assumed by 20.1 and 21.1 mA/cm^2 for 100 and 70 nm of CdS thickness. As it is seen, an increase in the resistivity ρ of the CdTe layer from 10^{-1} to 10^4 Ω cm leads to decreasing the open-circuit voltage V_o from 0.863 to 0.745 V at d_{CdS}= 100. The sharp increase in V_o at ρ = 0.1 Ω cm in comparison with large ρ is explained by the fact $\Delta\mu$ increasing with ρ, while the barrier for electrons lowers during their drift from CdS to CdTe. Besides, with decreasing the CdS thickness to 70 nm the same shape of the above curves can be observed.

The operating regime of the solar cell is the range of bias, from 0 to V_o, in which the cell delivers power. The cell power density is given by:

$$P = V\ J \tag{20}$$

P reaches a maximum at the cell's operating point or maximum power point. This occurs at some voltage V_m with a corresponding current density J_m and can be given by the maximum area that can be fitted between the x and y-axis of the illuminated *J-V* curve.

$$P_{max} = V_m\, J_m \tag{21}$$

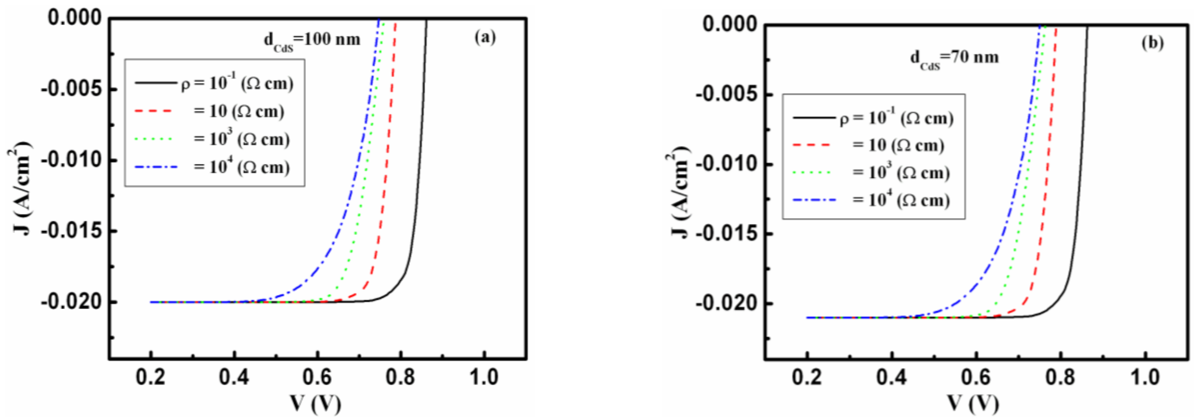

Fig. 4. J–V characteristics of CdS/CdTe heterojunction at different resistivities of the CdTe absorber layer at CdS thickness of 100 nm (a) and 70 nm (b).

Fig. (5) shows the dependence of the output power on the applied voltage of CdS/CdTe heterojunction at different resistivities of the CdTe absorber layer and thicknesses of CdS. It is clear that the output power increases with decreasing both the CdTe resistivity and at CdS thickness.

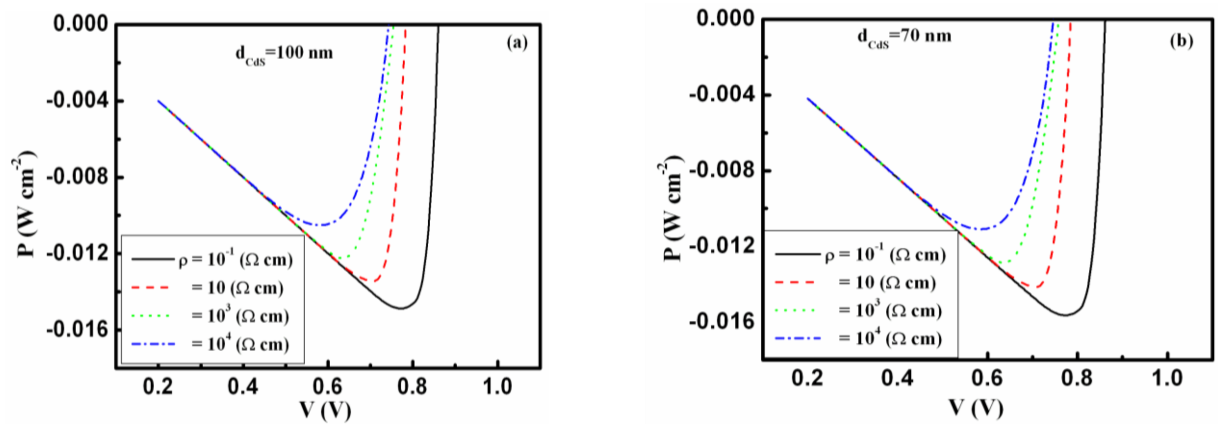

Fig. 5. Voltage dependence of the output power (P) of CdS/CdTe heterojunction as a function of different resistivities of the CdTe absorber layer at CdS thickness of 100 nm (a) and 70 nm (b).

The fill factor is defined as the ratio

$$FF = \frac{V_m\, J_m}{V_o\, J_{Sc}} \tag{22}$$

Fig. 6 shows the dependence of fill factor on CdTe resistivity at thickness 70 and 100 nm of CdS layer. As it is seen, the fill factor decreases from 0.864 to 0.687 with increasing the ρ from 0.1 to 10^4 Ω. On the other hand, the fill factor is weakly depending on the CdS thickness.

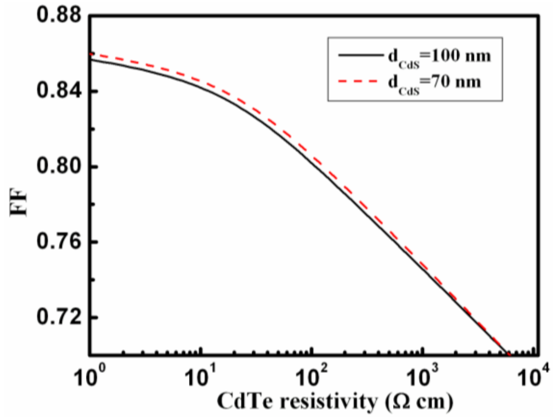

Fig. 6. Dependence of fill factor (FF) of CdS/CdTe heterojunction on CdTe resistivity at different thicknesses of CdS window layer.

Finally, the dependences of the efficiency $\eta=P_{max}/P_{inc}$ on the CdTe resistivity for various thicknesses of CdS layer is shown in Fig. 7, where P_{inc} is the density of the total AM 1.5 solar radiation power over the spectral range $h\nu \geq E_{gCdTe}$=1.46 eV equals 96.3 mW/cm^2 [25]. As it is seen, the value of η remarkably decreases from 15.48% to 10.6 % with increasing ρ from 0.1 to 10^4 Ω cm. With lowering the CdS thickness to 70 nm, a maximum efficiency of 16.5% is obtained at ρ=0.1 Ω cm. The calculated results turn out to be quite close to the efficiencies of the best samples of thin-film CdS/CdTe solar cells (16–17%) [10, 26-28].

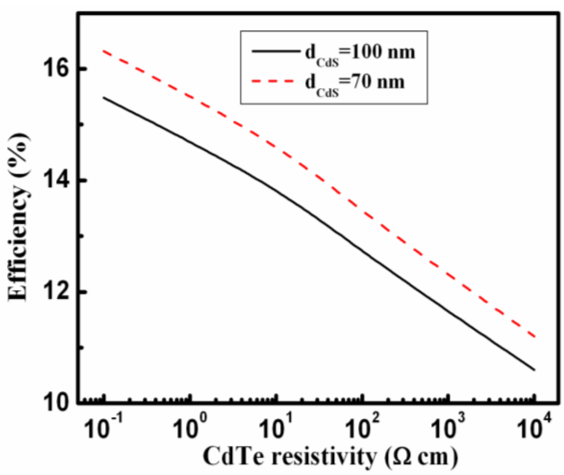

Fig. 7. Efficiency of CdS/CdTe cell versus CdTe resistivity at different thicknesses of CdS window layer.

5. Conclusions

The dependence of the short-circuit current, output power, open-circuit voltage and fill factor of a CdS/CdTe solar cell on the resistivity of the CdTe absorber layer and thickness of CdS window layer is studied theoretically in this work in order to enhance the cell efficiency. The calculations are carried out based on the optical (reflection and absorption) and recombination (front and back) losses under cretin parameters of the absorber layer. Reducing the CdS thickness from 100 to 70 nm leads to decrease the optical and recombination losses from 35% to 32% where the recorded maximum current density is 20.1 mA/cm^2 and 21.1 mA/cm^2, respectively. Both the CdTe resistivity and CdS thickness have remarkable effect on output power; fill factor and open-circuit voltage. These quantities increase with decreasing the resistivity of CdTe absorber layer and thinning the CdS layer. High efficiency of 16.5% is yielded at optimum conditions such as: CdTe thickness=5 μm; carrier lifetime (τ)=10^{-9} s; concentration of uncompensated acceptors (N_a-N_d)=10^{16} cm^{-3}; velocity of recombination at the front surface (S) and at back surface (S_b) of CdTe layer=10^7 cm/s; CdS thickness=70 nm and CdTe resistivity=0.1 Ω cm**.**

Acknowledgment

The author would like to thank the Deanship of scientific research, King Saud University ,Riyadh Saudi Arabia ,for funding and supporting this research. The author would like to acknowledge Prof. Dr. Leonid Kosyachenko for his help and cooperation during this work.

References

[1] V. Krishnakumar, J. Han, A. Klein, W. Jaegermann, Thin Solid Films, **519**, 7138 (2011).
[2] A. Y. Jaber, S. N. Alamri, M. S. Aida, Thin Solid Films, **520**, 3485(2012).
[3] R. Mendoza-Perez, J. Sastre-Hernandez, G. Contreras-Puente, O. Vigil-Galan, Sol. Energy Mater. Sol. Cells, **93**, 79 (2009).
[4] X. Wu, J. Zhou, A. Duda, Y. Yan, G. Teeter, S. Asher, W. K. Metzger, S. Demtsu, S.H. Wei, R. Noufi, Thin Solid Films, **515**, 5798 (2007).
[5] A. Kosyachenko, E. V. Grushko, X. Mathew, Sol. Energy Mater. Sol. Cells, **96**, 231 (2012).
[6] H. Yun, K. H. Kim, D. Y. Lee, B. T. Ahn, Sol. Energy Mater. Sol. Cells, **75**, 203 (2003).
[7] B. T. Ahn, J. H. Yun, E. S. Cha, K. C. Park, Current Applied Physics, **12**, 17 (2012)
[8] L. Kranz, J. Perrenoud, F. Pianezzi, C. Gretener, P. Rossbach, S. Buecheler, A. N. Tiwari, Sol. Energy Mater. Sol. Cells, **105**, 213 (2012).
[9] H. Zhao, A. Farah, D. Morel, C. S. Ferekides, Thin Solid Films, **517**, 2365 (2009).
[10] S. Chun , S. Lee , Y. Jung , J. S. Bae , J. Kim , D. Kim, Current Applied Physics, **13**, 211 (2013).
[11] First Solar Inc. website at: /http://www.firstsolar.com/S.
[12] S. Sze, Physics of Semiconductor Devices, 2nd ed., Wiley, New York, 1981.
[13] L. A. Kosyachenko, A. I. Savchuk, E. V. Grushko, Thin Solid Films, **517**, 2386 (2009).

[14] J. R. Sites, Sol. Energy Mater. Sol. Cells, **75**, 243 (2003).
[15] H. A. Mohamed, J. App. Phys., **113**, 093105 (2013).
[16] H. A. Mohamed, to be published in Canadian Journal of Physics, 2014.
[17] V. Ya. Roshko, L. A. Kosyachenko, E. V. Grushko, Acta Phys. Pol., A 120 (2011).
[18] B. A. Korevaar, A. Halverson, J. Cao, J. Choi, C. Collazo-Davila, W. Huber, Thin Solid Films, **535,** 229(2013).
[19] V. V. Brus, Sol. Energy, **86**, 786 (2012).
[20] Reference Solar Spectral Irradiance at the Ground at Different Receiving Conditions, Standard of International Organization for Standardization ISO 9845-1, 1992.
[21] C. Sah, R. Noyce, W. Shokley, Proc. IRE, **45**, 1228 (1957).
[22] L. A. Kosyachenko, V. M. Sklyarchuk, O. F. Sklyarchuk, V. A. Gnatyuk, Semicond. Sci.Technol., **22**, 911 (2007).
[23] L. A. Kosyachenko, I. M. Rarenko, Z. I. Zakharuk, V. M. Sklyarchuk, O. F. Sklyarchuk, I. V. Kabanova, O. L. Maslyanchuk, Semiconductors, **37**, 238 (2003).
[24] L. A. Kosyachenko, V. M. Sklyarchuk, O. F. Sklyarchuk, O. L. Maslyanchuk, V. A. Gnatyuk, T. Aoki, IEEE Transactions on Nuclear Science, **56**, 1827 (2009).
[25] T. Toshifumi, S. Adachi, H. Nakanishi, K. Ohtsuka, Jpn. Appl. Phys., **32**, 3496 (1993).
[26] J. Britt, C. Ferekides, Appl. Phys. Lett., **62**, 2851 (1993).
[27] A. Hanafusa, T. Hibino, K. Omura, H. Ohyama, M. Murozono, Jpn. J. Appl. Phys. 36, 6304(1997).
[28] P. V. Meyers, S. P. Albright, Prog. Photovolt. Res. Appl., **8**, 161 (2000).

*Corresponding author: hussein_abdelhafez2000@yahoo.com